International Journal of Applied Pharmaceutics

ISSN- 0975-7058 Vol 16, Issue 5, 2024

Original Article

FORMULATION AND EVALUATION OF ETODOLAC AND TRIAMCINOLONE ACETONIDE LOADED NANO LIPID CARRIER GELS FOR THE THERAPEUTIC MANAGEMENT OF OSTEOARTHRITIS PAIN THROUGH TOPICAL ADMINISTRATION: A COMPARATIVE STUDY

SOUVIK CHAKRABORTY[1], N. VISHAL GUPTA[2*], VIKAS JAIN[2], BALAMURALIDHARA V.[2]

[1]Department of Pharmaceutics, Eminent College of Pharmaceutical Technology, Mos pukur, Barbaria, Paschim Khilkapur, Barasat, Jagannathpur, West Bengal-700126, India. [2]Department of Pharmaceutics, JSS College of Pharmacy, Sri Shivarathreeshwara Nagara, JSS Academy of Higher Education and Research, Sri Shivarathreeshwara Nagara, Mysuru-570015, Karnataka, India
[*]Corresponding author: N. Vishal Gupta; [*]Email: vkguptajss@gmail.com

Received: 06 May 2024, Revised and Accepted: 21 Jun 2024

ABSTRACT

Objective: The present study aims to prepare carbopol-based hydrogels loaded with Etodolac (EDT), and Triamcinolone Acetonide (TCA) incorporated Nanolipid Carriers (NLCs) (EDTg and TCAg) to compare the efficacy and potency of both drugs for Osteoarthritis (OA) pain management.

Methods: EDT-NLCs and TCA-NLCs were prepared with the help of the solvent evaporation method after screening the lipids, and the NLCs were optimized. The optimized NLC formulations EDT-NLC and TCA-NLCs were examined for particle size, PDI, zeta otential, Differential Scanning Calorimetry (DSC), Powder X-ray Diffraction (PXRD), Transmission Electron Mcroscopy (TEM) and *in vitro* release. The prepared EDTg and TCAg have been evaluated with *in vitro* drug release, *ex-vivo* skin permeation, and *in vivo* pharmacokinetic and pharmacodynamic parameters.

Results: DSC and PXRD graphs showed a decrease in melting point and the amorphous form of the optimized NLC formulation. Different evaluation tests revealed that the EDT-NLCs and TCA-NLCshad particle size of 161±0.0021 nm and 167.4±0.0010 nm, PDI of 0.148±0.023 and 0.130±0.01, and zeta potential of-14 mV and-15 mV respectively, indicating their distinct nature. *In vitro* drug release study, ETDg showed 89.84±1.71 % release, while TCAg released 94.75±1.79 % after 24 h of application. ETDg permeated 86.5±1.68% of EDT-NLCs through the dorsal skin, compared to TCA-NLCs 76.5±1.13 %in an *ex vivo* skin permeation investigation. A pharmacokinetic study identified 76.3±1.98 % of EDT-NLCs and 63.25±2.003 of TCA-NLCs in drug plasma. Pharmacodynamic characteristics like X-ray analysis, Immuno Histochemistry (IHC), and histopathology indicated that EDTg and TCAg managed OA pain. All evaluation tests carried out in this research showed that formulated hydrogels could manage OA.

Conclusion: The results suggested in this research prove EDTg to have a higher potentiality than TCAg for the management of OA pain

Keywords: EDT, TCA, OA, NLCs, Hydrogels

DOI: https://dx.doi.org/10.22159/ijap.2024v16i5.51326 Journal homepage: https://innovareacademics.in/journals/index.php/ijap

INTRODUCTION

Osteoarthritis (OA) is a prevalent type of arthritis characterized by a complicated degenerative illness of the entire joint system that causes persistent difficulties in older adults [1]. These are characterized by cartilage deterioration, increased subchondral bone thickness, synovial membrane inflammation, and structural changes in various elements of the joints, such as the joint capsule, ligaments, and related muscles [2]. As a prevalent and disabling disorder, it increases the health burden with significant implications for people affected by this disease, as well as the socioeconomic expenses [3]. Unfortunately, the use of long-term analgesics and opioids is minimal, and there are no modifying therapies available for the treatment of the disease at the current end-stage, except total joint replacement surgery, which is inconvenient for many patients and may be an expensive affair for the patients to afford. Nonsteroidal Anti-Inflammatory Drugs (NSAIDs) and corticosteroids are the better classes of drugs for the treatment of OA pain. NSAIDs are currently indicated as an essential class of drugs for the frontline pharmacological therapy of OA pain [4, 5]. Some kinds of pharmacological treatment for OA include the administration of NSAIDs orally and topically, as well as intra-articular injections [6-8]. However, there are several risk factors associated with oral NSAIDs, including hepatotoxicity, renal failure with impaired kidney function, and adverse effects on the upper Gastro-Intestinal Tract (GIT), such as mild dyspepsia and heartburn, which may increase the complications of peptic ulcers in patients [9, 10]. Zeng and associates [11] conducted a systemic review of these parameters in which transdermal administration of NSAIDs is a safer alternative to oral administration and provides good pain relief. Corticosteroids have been used for decades to treat OA pain with Intra-Articular (IA) injections, providing short-term pain relief [12]. Intra-articular injections are also a painful treatment option for people with advanced OA. Repetitive corticosteroid IA injections may also raise the risk of infection, and long-term corticosteroid use has been proven to harm articular cartilage and accelerate joint deterioration. Transdermal Drug Delivery System (TDDS) or topical routes is a non-surgical and patient-friendly method for administering NSAIDs and corticosteroid-type drugs into the patient's body and providing delivery of drugs at the target site in a sustained manner; thus, long-term applicationsare possible without disrupting the patient's GIT and overcoming any skin infection caused by IA injections [13]. However, various challenges, such as the skin's barrier, as well as various body sites like Stratum Corneum (SC), which plays a crucial role in controlling the insurgence of the drugs and other chemical properties to pass through the skin to reach the site of action through the skin.

Because of the higher molecular weight of several NSAIDs and corticosteroid drugs, delivery through the SC region may be challenging for these drugs to reach their sites of action. In this situation, these drugs can be integrated with nanomaterials to provide potent drug administration through the skin while simultaneously limiting drug loss [14]. Nanomaterials are nanostructured units with unique properties that can be quantified in a single dimension using a nanometric scale. NLCs can prolong the contact time of the drug with the skin when given through a topical route to provide sustained drug delivery while improving the stability of the incorporated drug because they are cheap, biocompatible, and have the ability to incorporate lipophilic and hydrophilic drugs [15-17]. Among many NSAIDs, Etodolac (EDT) is the first-line NSAIDs class of drug used for the management of OA. This drug is composed of monocarboxylic acids, is approved for OA pain management, and can be used for long-term use to control the

signs and symptoms of the disease [18]. From various corticosteroid drugs, Triamcinolone Acetonide (TCA) is a potent drug candidate which can be injected into the patient's bloodstream via IA injections to alleviate the symptoms of OA pain [19]. Multiple TCA injections for long-term systemic usage will raise the risk of infections as well as the possibility of overdosing, which will result in unnatural adverse effects [20].

To overcome the challenges mentioned above faced by EDT and TCA during administration into OA patients, we have formulated topical gels containing NLCs loaded with EDT and TCA to provide an anti-inflammatory effect associated with OA pain. This study also compares the efficacy of EDTg and TCAg for a better understanding of which of the formulations provide a better effect. EDT-NLCs and TCA-NLCs were characterized extensively with the help of differential scanning calorimetry, X-ray diffraction and transmission electron microscopy, particle size analysis, PDI and zeta potential assay. *In vitro* drug releasestudieshave been conducted to evaluate the release profile of the drug from formulated NLCs. Finally, the EDTg and TCAg wereanalyzedwith specific*in vivo* parameters to determine their effects against inflammation in the induced Rat model.

MATERIALS AND METHODS

Materials

EDT and TCA were obtained as gift samples from Global Pharma (Global Pharma, Chennai, Tamil Nadu, India) and Sunvik Pharma (Sunvik Pharma, Chennai, Tamil Nadu, India). Compitrol ATO 888, glyceryl behenate, cetyl palmitate, and stearic acid, along with labrasol, labrafac PG, soyabean oil, oleic acid and Transcutol P, were received as a gift sample from Gattefosse (Gattefosse, Mumbai, India); Tween 80, pluronic F127, and span 80 were purchased from Quality Deal India (QDSI, Hyderabad, Telangana, India); Cabopol was gifted by Guapha pharmaceutical India

Methodology

Determination of λmax and calibration graph by High-Performance Liquid Chromatography (HPLC) method

The λmax values of EDT and TCA were obtained by dissolving them in methanol and measuring the wavelengths using Ultraviolet Visible (UV) spectrophotometry within the 400 to 200 nm range. The HPLC) method determined the drug content. A mobile phase was made for both drugs, consisting of 600 ml of acetonitrile and 400 ml of methanol each, which were mixed well under a water bath for 15 min. Both solutions were filtered through 0.45 µm under vacuum using the ultrapore filtration assembly. A C-18 column (25 cm × 4.6 mm, 5 µm) has been used for the pure drug, keeping a flow rate of 1 ml/min and the wavelength at 274 nm for EDT and 239 nm for TCA. Solution AE and solution AT have been prepared by dissolving 1 mg of pure EDT and TCA into methanol (0.1 ml) separately. The pure drugs ' stock solution (1 mg/ml) has been prepared by diluting AE and AT into the mobile phase solution. The HPLC column was injected with different solutions and was further analyzed (LC-2030C, Shimadzu, Japan) [21].

Estimation of EDT and TCA by liquid chromatography-mass spectroscopy (LC-MS) method

EDT and TCA drug plasma concentrations were detected using the LC-MS method on Acquity H-class UPLC (Waters Corporation, Milford, MA, USA). The BEH C18 column (2.1×50 mm, 1.7 µm) was used for the LC condition, and the temperature was maintained at 25 °C. 0.3 ml/min is the flow rate, and 5 µL of the sample was injected into the column. The solution of 0.1% formic acid in water has been considered the first mobile phase (A), and acetonitrile is regarded as the second mobile phase (B). With the gradient elution method, at 10, 20, 40, and 50, different ratios of A and B mobile phases have been injected into the column (5:95; 90:10; 95:5; 10:90). For MS conditions, an electrospray ionization (ESI) ion source has been used for negative ion mode detection with a voltage of 4 kV. The sheath temperature was kept at 350 °C, and the voltage for the tube and the capillaries was maintained at 110 V and 3000 V, respectively. The sheath and auxiliary gas flow rates have been kept at 40 l/h and 20 l/h, respectively, with a scan range of 50–1500 Da. All data were collected and processed using Xcalibur Data Acquisition and Interpretation Software [22, 23].

Experimental design

Screening of lipids and surfactants

In this method, the solid lipid, liquid lipid, and surfactant selection have been carried out according to the solubility of the EDT and TCA drugs into different lipid and surfactant samples. Compritol 888 ATO, glyceryl behenate, cetyl palmitate, and stearic acid have been chosen to screen solid lipids for NLC preparation [24, 25]. Liquid lipids such as labrasol, labrafac PG, soyabean oil, and oleic acid were chosen to prepare NLCs [26]. The solid lipids have been melted at 70 °C, and an increased amount of drug (mg) has been added to 1 g of lipid in a centrifuge tube. The same has been done for the liquid without heating, for it is already liquid. At 37 °C in a water bath shaker, the tubes containing the drug in solid and liquid were shaken for 48 h. According to the solubility of the drug, the amount of solid lipid and liquid lipid have been selected. Surfactants were chosen by mixing the EDT and TCA in an increasing order of 1 mg until they were undissolved in the molten surfactants. Tween 80, Pluronic F127, and Span 80 have been used as possible surfactants to prepare NLCs.

Preparation of EDT-NLCs and TCA-NLCs

Ten NLC formulations have been made for each drug (EDT and TCA) with other ingredients like Compritol 888 ATO, Labrasol, and Tween 80 (solid lipid, liquid lipid, and surfactant). These were made using the hot homogenization method and ultrasonication [27]. The preparation of NLCs has been divided into four stages. In stage 1, solid and liquid lipids were mixed under heating at 70 °C to form a lipid solution. A weight of 10 mg of drugs wascombined in the melted lipid solution. The surfactantwas mixed in 10 ml of millipore water in a separate beaker and kept for stirring in a magnetic stirrer at 15000 rpm at 70 °C to equalize the temperature with the drug-lipid solution. This procedure was performedon both drugs simultaneously. In stage 2, the drug-lipid solution was added to the surfactant solution dropwise, under continuous stirring. In stage 3, the lipid and surfactant mixture were homogenized at 10000 rpm under room temperature for 15 min. After homogenization, the prepared NLCs were kept aside for a few minutes and then taken for ultrasonification for 5–10 min in stage 4.

Preparation of EDTg and TCAg

NLC-loaded gels were formulated by preparing a gel base with 500 mg of carbopol 934 powder (gelling agent), soaked in 100 ml of distilled water, and continuously stirred for 15 min at 2000 rpm. To maintain the stability of the optimized NLCs, triethanolamine, an organic base, has been mixed with the gel base, which acts as a neutralizing agent. Optimized NLCs were centrifuged for 60 min at 12500 rpm. 5 ml deionized water was mixed to separate the optimized NLCs, and the supernatant was discarded. 10 ml of drug-loaded NLCs were added to the carbopol 934 gel base with continuous mixing at 2000 rpm for 10 min. Since the gels have been prepared for topical delivery, 5 % of Tanscutol P has been added to each formulation [28].

Characterization of prepared NLCs

Determination of particle size, PDI and zeta potential

A Nano-ZS Zetasizer (Malvern Instruments Ltd., Worcestershire, UK) has been employed to estimate mean particle size and PDI for the EDT-NLCs and TCA-NLCs. Approximately 1 ml of the sample was diluted in 10 ml of Millipore water and observed under light for blue tinge solution to ensure suitable scattering intensity before placing it into a 10×10×45 mm cell for PS analysis. Keeping the 900 nm scattering angle at 20 °C, the measurements were taken in replicates (n = 10). Mie theory has been utilised to analyse particle size data, with the absolute indices at 1.456 and the imaginary refractive indices at 0.01. Similarly, for the estimation of zeta potential, 1 ml of formulation was dissolved in 10 ml of Millipore water and placed into folded capillary cells. With the Helmholtz-Smoluchowsky equation *in-situ*, zeta poential for each sample was estimated at a field strength of 20 V/cm [29, 30].

Drug entrapment efficiency study (%EE)

For the estimation of %EE of the prepared EDT-NLCs and TCA-NLCs, an equal quantity of the pure form of the drugs and their formulated NLCs (1 mg) were centrifuged for 30 min at 4 °C by an ultracentrifuge (11.570 RCF). The supernatant was extracted and appropriately diluted in methanol to estimate the free drug present. The HPLC method has been used for analyzing the diluted samples [31]. The following equation has been used to quantify entrapped drug and drug-loading capacity:

$$\%EE = (W_a\text{-}W_s)/(W_a \times 100)$$

Where W_a is the weight of EDT added to the NLCs, W_s is the weight of EDT present in the supernatant post centrifugation.

Thermal analysis by DSC

DSC has been carried out for the determination of the melting point of the pure form of EDT and TCA drugs, EDT-NLCs, TCA-NLCs, and the physical mixture to check the compatibility between the drugs and the other excipients of the prepared nanoformulation. The DSC-60 instrument (Shimadzu Corporation, Tokyo, Japan) has been used to conduct this study [32]. Measurements from calorimetry were done using empty cells made up of high-purity alpha-alumina discs as the reference and a pan press was performed. Spectral measurements were obtained on DSC-60 at a 20–300 °C temperature range.

Crystallographic analysis and PXRD

To identify the crystallinity or amorphous form of the formulated NLCs, PXRD has been used (X'PERT PRO SUPER, Panalytica, Holland), where scanning of the pure drug samples, the physical mixture of the compounds, and the formulated NLCs have been done over a 2θ range (5–50°) at a scan rate of 0.05°/s with the help of Cu Kα radiation. The PXRD graphs for the NLCs were compared with the graphs of the drug and the physical mixture to observe the drug's primary form and the prepared formulation [33].

Morphology of EDT-NLCs and TCA-NLCs by TEM

The morphological conditions of the prepared NLCs containing EDT and TCA have been carried out with TEM (JEM-1200EX, JEOL). Double-sided adhesive tape was placedin the analytical test region of the sample. Samples of the prepared NLCs have been made by diluting them in double-distilled water and placing a formulation drop on a carbon film-coated 400-mesh copper grid. Negative staining has been done with 1% phosphotungstic acid for proper visualization under the microscope [34].

Evaluation tests for EDT-NLCs and TCA-NLCs

***In vitro* drug release study**

In vitro release of EDT-NLCs and TCA-NLCs has been carried out with the help of a dialysis bag at ambient temperature [35]. For this study, four open-end test tubes were taken and mounted with dialysis membranes with a pour size of 2.4 metres at one side of the tubes. Two tubes each got 2 ml (1 mg) of pure EDT and TCA dispersions, and the other two tubes each got 5 ml of EDT-NLCs and TCA-NLCs (Himedia-Dialysis Membrane 135, Mol. cut off 12000–14000 Da, Mumbai, India). The dialysis bag was submerged in beakers comprising 100 ml of saline phosphate buffer (PBS) pH 6.8 (receptor compartment). PBS was kept stirring at a speed of 600 rpm at room temperature. At different time intervals, 5 ml of each drug sample was withdrawn with the help of a syringe for drug content analysis by HPLC method.

Stability study

For stability studies, lyophilized samples of the optimized EDT-NLCs and TCA-NLCs were stored at 4 °C and 25 °C. At different time intervals (days 0, 7, 15, 30, and 60), the dry samples were diluted in water, and various parameters such as particle size, PDI, and zeta potential were measured [27].

Evaluation tests of EDT-NLCs gel and TCA-NLCs gel

Determination of pH

pH of the formulated EDT-NLCs (EDTg) and TCA-NLCs gels (TCAg)were determined by mixing 1 ml of NLCs in distilled water (10% w/v). pH of the mixture was recorded with the help of a pre-calibrated pH meter electrode (PHS-3BW, Biobase, China) immersed into the prepared gels. The experiment was conducted in triplicate [36].

Viscosity analysis

The prepared EDTg and TCAg viscosity were evaluated using a Brookfield viscometer (Brookfield DV2T Viscometers, Brookfield, India). The SC4-27 spindle had been used to operate at 100 rpm, and the viscosity was analysed at a temperature of 25±0.1 °C. The experiment was conducted in triplicate [36].

***In vitro* drug release study**

The drug release study for the formulation has been carried out using the dialysis sac method. Withdrawn samples were analyzed with the help of the HPLC method [37].

***Ex vivo* skin permeation study**

This study aimed to predict the delivery and drug permeation of EDT-NLCs and TCA-NLCs from the formulated EDTg and TCAgthrough the skin surface into the site of action. Skin from the dorsal area of the rats has been taken and preserved in a formalin solution for 24 h. A modified trans-diffusion cell apparatus has been used on which isolated rat skin was mounted, keeping the epidermal layer facing towards the donor compartment. 6.8 pH PBS was taken as a receptor medium at a maintained temperature of 37± 0.5 °C. The medium was kept for stirring at a speed of 300 rpm. Formulated EDTg and TCAgwere placed on the skin's epidermal surface in the donor compartment. 5 ml of PBS solution was withdrawn at pre-determined intervals (1, 2, 4, 6, 8, 12, 24 h). With the help of the HPLC method, all samples were analyzed for NLC gels [38-40]. *In vitro* percutaneous flux ($\mu g/cm^2 \times h^{-1}$) of EDT NLCs and TCA-NLCs was calculated with the help of a graph, taking the cumulative amount of NLCs permeated through the skin at the y-axis and time at the x-axis. The determination of steady-state permeation flux has been observed from the slope of the linear portion of the cumulative amount of permeated ($\mu g/cm^2$) versus the time (h) plot.

$$\text{Flux (J)} = M/t$$

Animal study

Animal

Thirty male rats (Albino Wistar; 250–300 gs) provided by Adita Biosys Pvt Ltd. (Tumkuru, Karnataka, India) were weighed and allocated into ten groups (3 rats per group) as per the weight of the animals for this study. Male rats have been taken into account in this study to estimate the high efficacy of the formulations for the therapy of OA. Animals were kept at optimum room temperature on a 12 h light/12 h dark cycle with a daily food and water supply. To diminish the pain or distress faced by the animals, suitable procedures were taken into account, and all experiments were carried out under the approved guidelines of the ethics committee of the Institutional Animal Ethics Committee (IAEC) and the principles of laboratory animal care. All the animals were given an acclimatization period of 7 d, after which the animal study commenced. All the animal studies have been carried out with the approval of the Institutional Animal Ethics Committee (IAEC) of JSS College of Pharmacy, Mysuru (JSSAHER/CPT/IAEC/070/2021).

Study design

The animals were grouped randomly, as tabulated in table 1, for pharmacokinetic and pharmacodynamic studies. The following groups, such as group I, have been considered a controlled group with no disease induction. In contrast, group II comprises untreated animals where MIA has been induced to form the OA. For pharmacokinetic study, groups III, IV, V and VI have been selected in which OA has not been caused. IngroupsIII and IV, animals were treated with EDT and TCA oral suspensions, respectively. Groups V and VI were treated with developed EDTg and TCAg, respectively. For the pharmacodynamic study, groupsVII, VIII, IX, and X consist of OA-induced animals,in which animals of group VII and VIII were treated with oral suspensions of EDT and TCA, respectively, andanimals of group IX and X weretreated with formulated EDTg and TCAg respectively.

Table 1: Grouping of animals used for pharmacodynamic and pharmacokinetic study

Groups	Number of animals	Method
Group I	3	Controlled (Without any induction of the disease)
Group II	3	Induced with OA without any treatment
Pharmacokinetic Study		
Group III	3	Treated with oral suspension of EDT
Group IV	3	Treated with oral suspension of TCA
Group V	3	Treated with EDTg
Group VI	3	Treated with TCAg
Pharmacodynamic study		
Group VII	3	Induced with OA and treated with Oral suspension of EDT.
Group VIII	3	Induced with OA and treated Oral suspension of TCA.`
Group IX	3	Induced with OA and treated with developed EDTg
Group X	3	Induced with OA and treated with developed TCAg

Pharmacokinetic (PK) study

For the estimation of EDT-NLCs and TCA-NLCs in the blood plasma from the formulated gels, a pharmacokinetic study has been conducted by collecting blood samples from the retro-orbital plexus of the rats post-anesthetization with diethyl ether. Plasma samples were separated by immediate centrifugation (VS-60ocFi, Korea) for 20 min at a speed of 3500 rpm and stored at-70 °C until further analysis [41]. The detection of EDT-NLCs and TCA-NLCs concentrations present in the plasma has been analyzed with the help of the LC-MS method. The pharmacokinetic parameters for the NLCs from the formulated gel and oral suspensions in the blood were designed with the help of standard non-compartmental methods. From a visual examination, the concentration of peak serum and the reaching time into the plasma (C_{max} and T_{max}) were evaluated and applied to determine the absorption rate. Linear regression of log-transformed data in the terminal phase of the concentration of the serum and the time profile has been applied for the determination of the elimination rate constant (K_{el} (h^{-1}) [42]. A quotient of 0.693/K_{el} (h^{-1}) has been used to determine the elimination half-life ($T_{1/2}$). A linear trapezoidal rule has been applied to estimate the area under the curve for the concentration-time (AUC_{0-t}) curve from the serum concentration from zero to the time of the last quantifiable concentration (C_t). The area under the serum concentration-time curve (AUC_{0-i}), which has been extrapolated to infinity, has been determined with the help of the following equation [43].

$$AUC_{0-I} = AUC_{0-t+}C_t/K_{el}$$

The pharmacokinetic profiles of EDT and TCA from the formulated gels have been compared, and the comparative bioavailability of the test or reference was calculated with the help of the following equation [42].

$$AUC_{0-t}\ (test)/AUC_{0-C}$$

Induction of monosodium iodoacetate (MIA) for OA formation

During the post-acclimatization period (1st d), OA was induced in the animals in the groups, as mentioned in table 1. After anaesthesia, with an equal amount of Xylazine and Ketamine, a single dose of Monosodium Iodo-Acetate (MIA), containing 3 mg of the drug, was dissolved in 50 µl of sterile saline and administered into the left knee of the animals through intra-articular injection [44] and kept for two weeks for the formation of OA [45].

Joint swelling measurement for osteoarthritis-induced rats

After two weeks, animals induced with OA started immovable activities such as limping and crawling, with minute swelling at the left knee joint. For measuring the joint volume at the knee area of the animal, a digital calliper has been used to calculate the swelling of the knee region. This process has been carried out throughout the experiment at a one-week interval [45].

Treatment of the animals

After two weeks, the animals groups IX and X (table 1) were treated with EDTg and TCAg, respectively, by applying formulated gels to the shaved knee region and covering them with an adhesive gauge for prevention. Animals of groups VII and VIII have received oral doses of EDT and TCA suspensions. Treatment was continued for 14 d with daily application of gels to the skin and drug suspensions through oral routes to the animals.

OA formation determination by X-ray

X-ray radiography has been conducted to compare the treatment between the groups of animals treated with the formulated gels and oral suspensions (group VII-X) to observe any changes in the animals' joints after treatment. Rats were anaesthetized using equal doses of xylazine and ketamine. The rats were kept on the X-ray plate and radiographed using a V-Xvue digital imaging system. Animals were anaesthetized and placed on the detector plate 30 inches from the X-ray emitter. The X-ray dose for the generator was set at kV (kVP = 70) and mAs (1.000) [46].

Histopathological parameters and IHC

Histopathology has been carried out to understand the morphology of different tissues of the animals collected, such as joints, skin, and spleen, post-administration of the drug by gels and oral suspension, and to study the effects of EDT and TCA. To estimate histopathological parameters, the left knee joints of the animals have been examined to observe any changes in the joints post-treatment. Spleen parts of the animals have also been dissected from the animals of every group to observe any infection due to the administration of the pure drug by oral suspension. Only the skin sections from groups IX and X to which developed gels have been applied. The lateral and medial sides of the femoral condyle and tibial plateau were fixed in PBS containing 70–90% alcohol for 7 h and decalcified in xylene and paraffin wax for 9 h. Decalcified tissues were cut into 5-micron-thick paraffin sections with tissues in the ribbon to be made with a Leica microtome. The ribbon will be floated in the 37 °C water bath, and the wax ribbon will be taken on glass slides. Slices were obtained and stained with hematoxylin and eosin (HandE). The sections were dehydrated using 3 concentrations of 80, 90, and 100% alcohols, cleared with 3 changes of xylene, and mounted with DPX [47].

IHC has been carried out to score or study the expressions of different antibodies, such as interleukin (IL)-1β, IL-6, and Tumour Necrosis Factor (TNF)-α, on the joints of the animals that were collected pre-analysis. For immunohistochemistry, the slices of the knee joints were rehydrated and incubated in 100% alcohol for 8 min. After trypsinization with peroxidase blocking using 3% hydrogen peroxide, sections were washed with distilled water and Phosphate Buffer Salione (PBS). The sections were blocked for 30 min at room temperature. The sections were incubated with primary antibodies with an appropriate dilution for 1 hour at room temperature or 4 °C overnight. The sections were rinsed with PBS and covered with appropriate secondary antibodies for 30 min. We washed with PBS again, and the slides were covered with DAB substrate (3,3′ -Diaminobenzidine) buffer with DAB chromagen. After 5 min, counterstaining with hematoxylin for 3 min was done, washed with tap water, and differentiated with 1% acid alcohol. ImageJ software has been used to obtain Immunohistochemistry (IHC) data, which were semi-quantitatively scored by calculating the intensity of the primary Interleukin (IL)-1β, 6, and Tumor Necrosis Factor (TNF)-α staining and the percentage of a positive detection, in

which the results were counted as score 1 showing regular expression of antibodies in joints (>25%), score 2 showing mild enhanced expression of antibodies in joints (25% to 50%), score 3 showing moderately expression of antibodies in joints (50–75%), and score 4 showing severe expression of antibodies in joints (75%–100%) [48].

Statistical analysis

All the data have been expressed as mean Standard Deviation (+SD). The experiments were performed by taking at least three replicates. For the statistical analysis, one-way and two-way ANOVA were utilized. Design of Experiments (Design-Expert, version 13.0, Stat-Ease, USA) software has been used for screening, optimization, and statistical treatment of formulation data with the help of Microsoft Excel.

RESULTS AND DISCUSSION

The λ_{max} of EDT and TCA in methanol was assessed in fig. 1. The chromatogram in fig. 2 displays the retention time for EDT at 6.574 min under the wavelength of 274 nm and the retention time for TCA at 4.018 min under the wavelength of 239 nm. For this reason, all the analytical parameters, such as *in vitro* drug release and ex vivo drug permeation studies, have been carried out at these wavelengths.

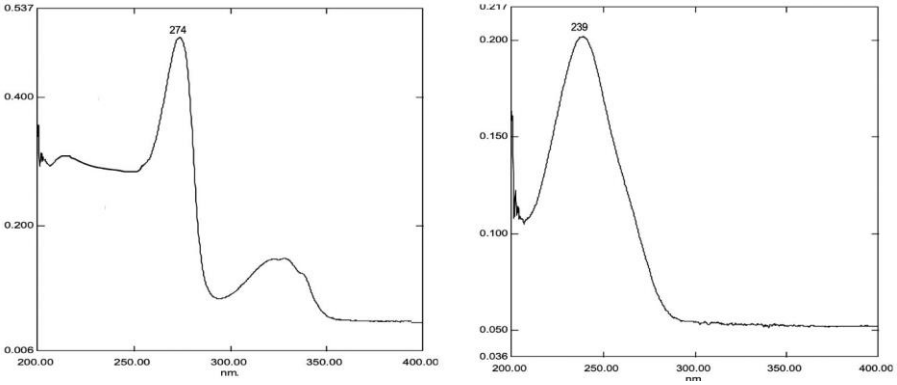

Fig. 1: UV spectrum of EDT and TCA in methanol

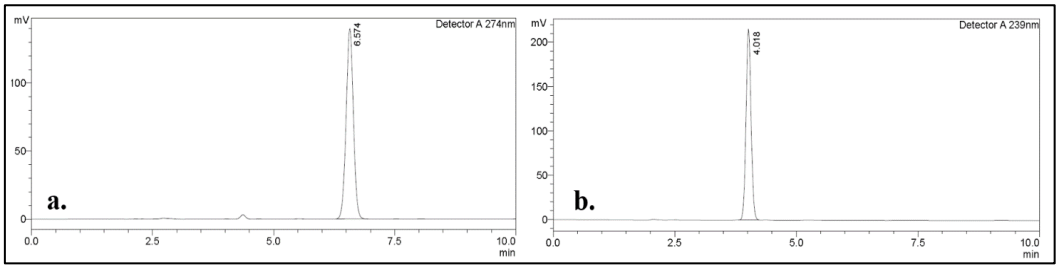

Fig. 2: HPLC chromatogram of (a.) EDT and (b.) TCA

The percentage concentration of the drug in the plasma was determined using the LC-MS method. Blank plasma samples were initially prepared from the blood of the animals in the negative control groups to ensure no interference from any endogenous compounds in the blood plasma. Seven concentrations of the homogenized plasma ranging from 10.0 to 1000.00 ng/ml have been considered for the calibration graph, constructed by plotting the peak area of the standard concentration at the x-axis and against their respective concentrations at the y-axis. Mass Selective Detector (MSD) was in fix-positive ionization mode with selected ion monitoring.

The R^2 of EDT from the equation y = 701.97x+6954.8 was found to be 0.9994. The retention time of the drug was determined to be 3.06 min. The concentration of the unknown samples was determined from the interpolation of the calibration curve (fig. 3).

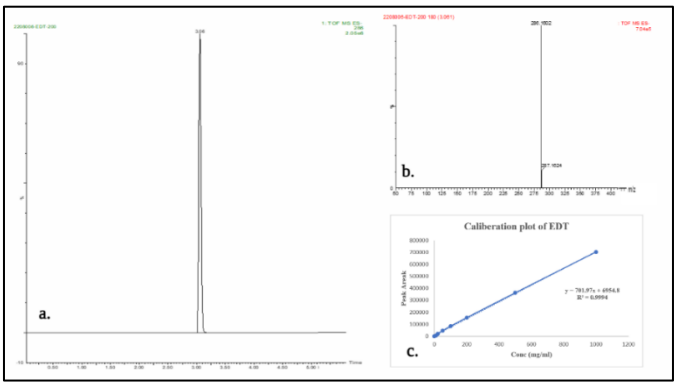

Fig. 3: LC-MSC linearity of EDT. (a.) Chromatogram for 200 mg/ml standard concentration with retention time 3.06 min, (b.) obtained from the analysis of EDT represented in m/z values and (c.) Calibration curve of EDT in triplicate

In the case of TCA, R^2 was found to be 0.999 from the equation y = 633.24x+12256. The retention time of the drug was determined to be 2.38 min. The concentration of the unknown samples was determined by interpolating the calibration curve (fig. 4).

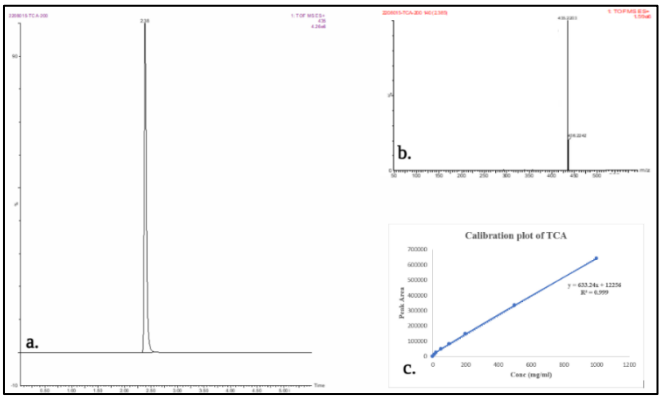

Fig. 4: LC-MSC linearity of TCA. (a.) Chromatogram for 200 mg/ml standard concentration with retention time 2.38 min, (b.) obtained from the analysis of TCA represented in m/z values and (c.)

The selection of solid lipid, liquid lipid, and surfactant is an essential and crucial factor for the formulation of NLCs. Among all the components used for screening tests, the highest solubility of EDT and TCA was found in Compritol 888 ATO (solid-lipid), Labrasol (liquid-lipid), and Tween 80 (surfactant). According to fig. 5, the lowest amounts of EDT and TCA have dissolved completely in Compritol 888 ATO, Labrasol, and Tween 80. For this reason, these components have been selected for further NLC formulation. The lipids and the surfactants were chosen for the preparation of NLCs by observing the solubility of the EDT and TCA drugs in various lipids and surfactants. Compritol 888 ATO, Labrasol, and Tween 80 could dissolve a lower amount because they had co-surfactant properties that reduced contact angle and interfacial tension, which solubilized the drug into the components [49-52].

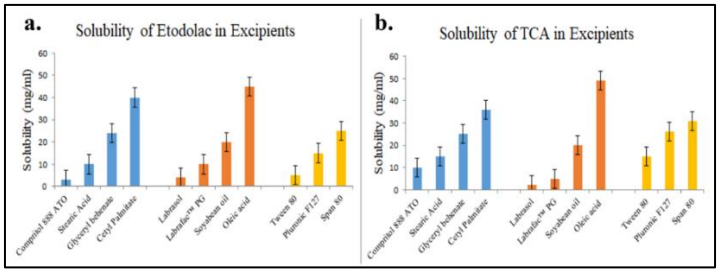

Fig. 5: Amount of (a.) EDT and (b.) TCA solubilised in Solid Lipid (■), Liquid Lipid (■) and Surfactant (■) used for the preparation of EDT-NLCs and TCA-NLCs, data represted as mean±SD, n = 3 observations

PS analysis have been done for the determination of the size of the NLCs of the particles in the nano-range [53,54]. According to the peak graph shown in fig. 6, the mean PS of the optimized formulation EDT-NLCs and TCA-NLCs were found at 161±0.021 nm and 167.4±0.101 nm, respectively, which revealed uniformity in particle distribution. The PDI of both NLCs was found to be 0.148±0.231 and 0.130±0.103. ZP peaks for the optimized formulation were-14±0.021 mV and-15±0.032 mV for the formulated EDT-NLCs and TCA-NLCs, respectively.

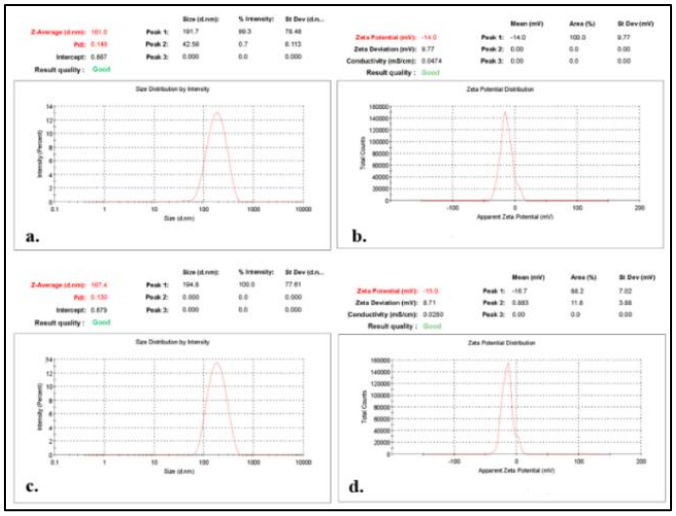

Fig. 6: (a.) PS and PDI of EDT-NLCs, (b.) ZP of EDT-NLCs, (c.) PS and PDI of TCA-NLCs and (d.) ZP of TCA-NLCs

About 87.38% of EDT and about 78.4% of TCA have been entrapped in prepared EDT-NLCs and TCA-NLCs due to the optimum levels of lipids and surfactants, which improve EE and drug content.

In DSC analysis, the endothermic peaks of pure drugs, EDT-NLCs, TCA-NLCs, and the physical mixture of the different components are shown in fig. 7. The DSC curve of the pure EDT and TCA exhibited an endothermic peak at 154 °C and 299 °C at an onset temperature of 151 °C and 290 °C, corresponding to their melting points. 103 °C has been observed for EDT-NLC at the onset of 98 °C. TCA-NLC showed a melting point of 76 °C at the onset of 72.46 °C. Meanwhile, endothermic peaks were observed for the physical mixture at 75 °C and 70 °C. The vast decline range in the melting points of formulated NLCs shows that the drugs have been wholly entrapped in the excipients, and there is no drug loss during the preparation period.

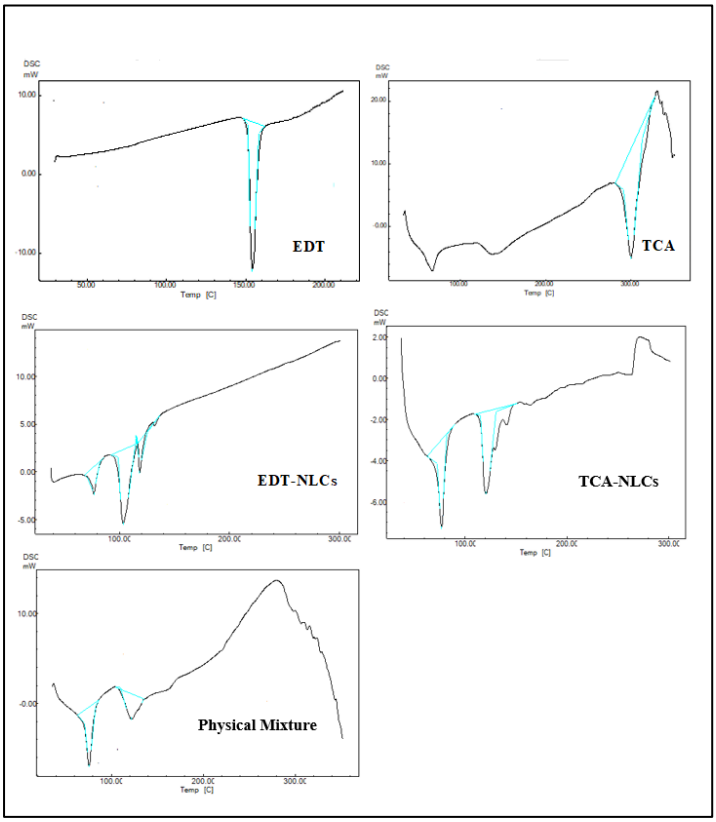

Fig. 7: DSC thermogram of EDT, TCA, EDT-NLCs, TCA-NLCs and physical mixture

The morphology and the structure of the for the prepared NLCs, along with obtained PS have been analyzed by TEM as shown in shown in fig. 8, which depicts that the NLCs had nanometer-size spherical shapes with no visibility of nanocrystals within the nano-sized range [55, 56].

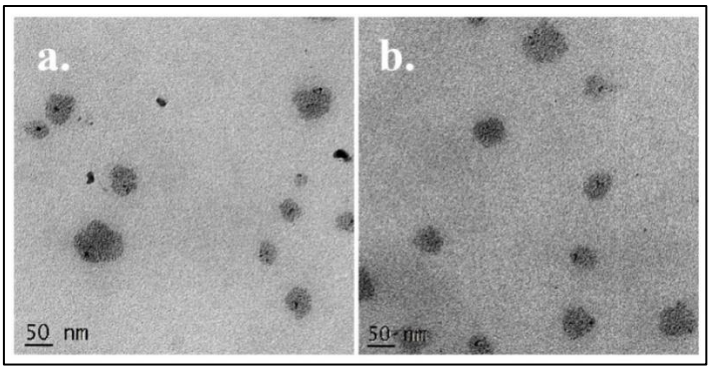

Fig. 8: TEM images of (a.) EDT-NLCs and (b.) TCA-NLCs

The PXRD graphs in fig. 9 depict the nature of the pure drugs, the prepared NLCs, and the physical mixture of the excipients. The XRD pattern for the pure EDT and TCA shows sharp peaks, depicting the pure drugs' crystalline nature, whereas the physical mixture pattern shows the amorphous nature of the excipients. The PXRD graph for the EDT-NLCs and TCA-NLCs depicts the amorphous nature of the prepared NLCs, which is somehow similar to that of the physical mixture, which proves complete entrapment of the drugs into the lipid and surfactant solutions. The amorphous nature of the formulated NLCs has been observed in PXRD reports, suggesting that the EDT and TCA were entrapped in their respective NLC formulations without any unentrapped crystalline drug residue [57].

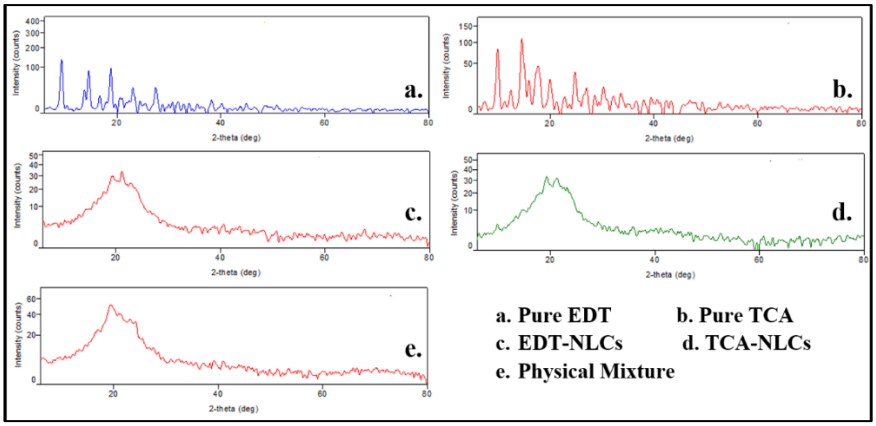

Fig. 9: PXRD graph for pure EDT and TCA with EDT-NLCs and TCA-NLCs and the physical mixture

In vitro drug release study were performed distinguish the amoun of EDT and TCA release from the respective formulated NLCs [58]. As per the *in vitro* drug release profile, a significant improvement in the release rate from the formulated NLCs has been observed compared to the suspension of the pure drug. Fig. 10 plots the release patterns of both NLCs and the pure forms of EDT and TCA. *The in vitro drug* release profile for the pure EDT showed a steep slope with 85.79±1.28 % of release after 10 h, indicating rapid release. In contrast, the release profile for EDT-NLCs showed a non-linear release pattern with 89.84±1.71 % release, exhibiting no burst behaviour and proving a sustained release. *The in vitro* drug release profile for the pure TCA also showed a steep slope with 91.27±1.47 % of release after 10 h, indicating rapid release. In contrast, the release profile for TCA-NLCs showed a non-linear release pattern with 94.75±1.79 % release, exhibiting no burst behaviour and proving a sustained release.

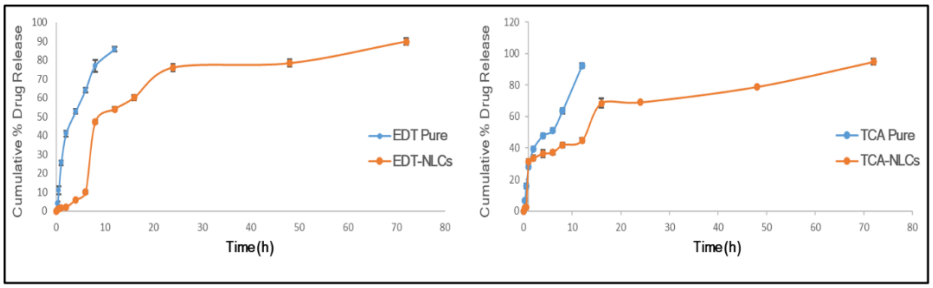

Fig. 10: *In vitro* drug release profile of (A.) pure EDT and EDT-NLCs, and (B.) pure TCA and TCA-NLCs, data represted as mean, n = 3 observations

A long-term physical stability study has been carried out for EDT-NLCs and TCA-NLCs by storing them for 60 d at 4 °C and 25 °C. Table 2 tabulates the stability of the prepared NLCs at different temperatures. Evaluation of particle size, PDI, and zeta potential of the prepared NLCs has been done to observe their potent stability. An increase in PS of EDT-NLCs has been observed from 161.0 nm to 175.6 nm at 4 °C, with an increase in the PDI from 0.148 to 0.286. The zeta potential of the EDT-NLCs gradually increased from-14 mV to-7.47 mV during the initial 60 d of stability testing. At 25 °C, there is an increase in particle size of the EDT-NLCs from 161 nm to 177.4 nm, an increase in PDI from 0.148 to 0.248, and a zeta potential increased from-14 mV to-7.03 mV. The PS gradually increases in both temperature points for 60 d, with a size range of 167.4 nm to 268 nm at 4 °C and 167.4 nm to 315 nm at 25 °C. The PDI of TCA-NLCs stored at 4 °C was found in the range of 0.13 to 0.209 and at 25 °C in the range of 0.13 to 0.269. The zeta potential for the TCA-NLCs is increasing at a rate of-15 mV to-6.3 mV at 4 °C and-15 mV to-5.2 mV at 25 °C. *In vitro* studies have revealed that both NLCs show controlled and higher biphasic drug release than the pure forms of the drugs (EDT and TCA) due to the encapsulation of the drugs in the outer layer of the lipids used, which facilitates a burst release [59].

Table 2: Stability study at different temperatures of EDT-NLCs and TCA-NLCs

EDT-NLCs	Days	Particle size (nm)		PDI		Zeta potential	
		at4 °C	at25 °C	at4 °C	at25 °C	at4 °C	at25 °C
	0	161±0.2	161±0.21	0.148±0.01	0.148±0.016	-14±0.2	-14±0.21
	7	170.1±1.2	170.5±0.6	0.196±0.008	0.198±0.001	-14.8±0.34	-15±0.25
	15	170.7±0.4	171.2±1.12	0.193±0.037	0.198±0.011	-9.77±0.07	-8.67±0.15
	30	174.2±2.8	175.5±1.06	0.206±0.006	0.208±0.034	-8.67±0.14	-7.88±0.23
	60	175.6±1.9	177.4±1.17	0.286±0.056	0.248±0.015	-7.87±0.31	-7.03±0.11
TCA-NLCs	0	167.4±0.21	167.4±2.1	0.13±1.1	0.13±1.1	-15±0.21	-15±0.21
	7	168.2±0.25	176.9±0.21	0.129±0.21	0.119±0.024	-14.8±0.021	-12.5±1.1
	15	176.5±0.32	184.5±0.36	0.154±0.25	0.192±1.26	-10.3±2.1	-9.4±2.6
	30	261±1.6	290±0.006	0.176±1.2	0.202±0.22	-9.8±0.33	-7.9±1.6
	60	269±2.2	315±0.034	0.209±0.012	0.269±0.15	-6.3±0.03	-5.2±0.13

Data represted as mean±SD, n = 3 observations, the pH of the resultant gel formulation was 6.52±0.1 and 6.86±0.25 for EDTg and TCAg, respectively, which is a suitable pH for topical products.

The viscosity of the prepared EDTg and TCAg was found to be 6831±2.47 cps and 6702±1.57 cps, respectively.

The cumulative percentage release of EDTg and TCAg were investigated for 24 h (fig. 11). Fraction drug release at the end of 24 h for EDTgwas found to be 86.5±1.68%, and for TCAg been found to be 76.5±1.13 %. In this study, we can observe that, after 24 h, EDTg produces higher drug release than the other TCAg.

% cumulative drug permeation of these gels has been carried out to compare the permeation of the NLCs through the dorsal skin of a rat. Further permeability of EDTg and TCAg was evaluated by measuring cumulative % drug permeated, steady state flux (J) and permeability coefficient documented in table 3. The drug permeation results plotted in fig. 12, we can observe that 76.08±1.56% EDT-NLCs have been permeated from EDTg and 65.31±2.1 % of TCA-NLC has been permeated from the TCAg after 24 h. The steady flux (J) after 24 h for EDTg and TCAg was found to be 15.85±0.25 µg/cm^2 × h^{-1} and 13.60±0.33 µg/cm^2 × h^{-1}.

The concentration vs. time graph for EDT oral suspension and EDTg, as well as TCA oral suspension and TCAg, is represented in fig. 13. The graphical representation showed 98.93±1.26 mg/ml of EDT in the blood plasma through oral administration, whereas the EDTg showed 76.3±1.98 mg/ml concentration in the blood plasma. For TCAg, 63.25±2.003 mg/ml concentration has been observed in the drug plasma, compared to TCA oral suspension, which showed 98.13±1.03 mg/ml concentration, administered through the oral route. Although the drug plasma level is lower through gels, there is a minimal amount of drug loss, which can be modified by customizing the ratio of adhesive polymers and increasing the concentration of the penetration enhancer. Comparatively, EDTg showed higher drug plasma concentrations than TCAg. The PK parameters were evaluated for oral suspension of EDT and TCA, EDTg, and TCAg, as outlined in table 4.

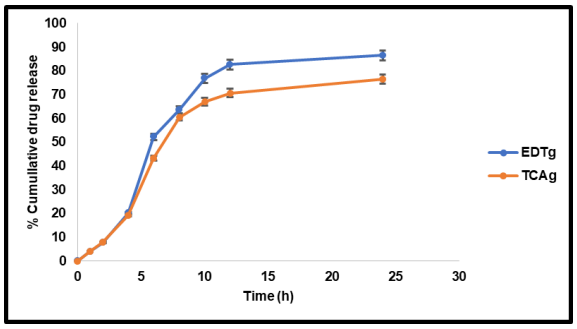

Fig. 11: *The in vitro* (%) drug release profile of EDTg and TCAg has been shown in graph, data represted as mean, n = 3 observations

Table 3: Cumulative % drug permeated, steady state flux (J) and permeability coefficient of EDTg and TCAg

Parameters	EDTg	TCAg
The cumulative amount of drug permeated at 24 h SD±3 (µg/cm^2)	76.08±1.56%	65.31±2.1 %
Steady-state flux across scleral tissue (J) SD±3 (µg/cm^2/h^{-1})	15.85±0.25	13.60±0.33
Permeability coefficient SD±3 (cm/h)	0.0158±2.55	0.0136±0.15

Data represted as mean±SD, n = 3 observations

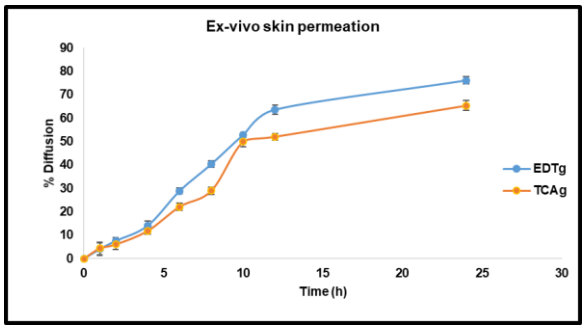

Fig. 12: *An ex vivo* (%) drug permeation study of EDTg and TCAg is shown in the graph, data represented as mean±SD, n = 3 observations

Table 4: PK parameters for EDT oral, TCA oral, EDTg, and TCAg in the plasma of the treated animal

PK parameters	EDT oral	EDTg	TCA oral	TCAg
Cmax (mg/ml)	98.93±1.26	76.3±1.98	98.13±1.03	63.25±2.003
Tmax (h)	6	12	4	12
Kel (h^{-1})	0.0174±0.0143	0.0254±0.0132	0.0096±0.00013	0.0143±0.000125
T1/2 (h)	39.73±0.0032	27.25±0.0135	71.83±0.0037	48.24±0.0021
AUC (0-24) (mg. h/ml)	1178.74±0.029	1087.95±0.025	801.73±0.012	762.99±0.023
AUC (24-∞) (mg. h/ml)	395.63±1.26	118.65±1.48	1075.64±1.02	164.89±1.43
AUC (0-∞) (mg. h/ml)	1574.37±0.035	1206.6±0.048	1877.37±0.032	909.89±0.021
AUMC (0-24) (mg. h^2/ml)	9650.66±0.048	5900.26±0.035	6009.77±0.023	4432.42±0.021
AUMC (24-∞) (mg. h^2/ml)	32180.36±0.169	7514.58±0.0188	137317.31±0.021	13751.94
AUMC (0-∞) (mg. h^2/ml)	41831.035±0.146	13414.75±0.154	143327.08±0.053	18184.37±0.041
MRT (0-∞) (h)	26.56±0.048	11.11±0.033	76.34±0.043	19.98±0.032
Relative Bioavailability	0.00922±0.059		0.0095±0.0041	

Data represted as mean±SD, n = 3 observations

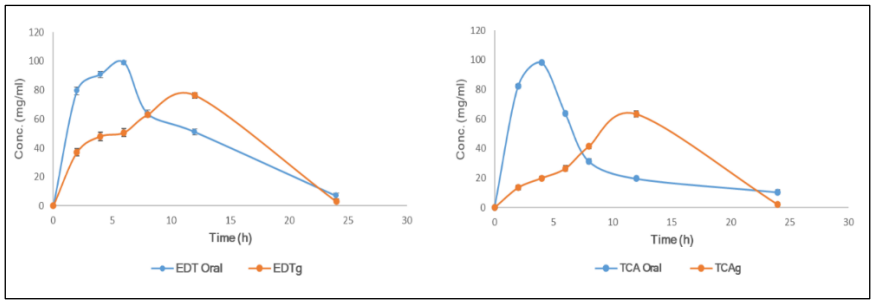

Fig. 12: Concentration versus time profile curve of (a.) EDT oral suspension through oral administration and EDTg, and (b.) TCA suspension through oral administration TCAg, data represted as mean, n = 3 observations

After the OA induction into the animal's left knee joint through intra-articular injection, the disease was treated according to the swelling index of the joint region at a maximum level. The volume of the knee joints was estimated for three groups after two weeks of disease induction. The change in the volume of the knee joints for all the animals in different groups was recorded after two weeks of treatment. Significant swelling of the knee joint volume for the controlled group, reaching up to 12±0.32–13.8±0.43 mm, has been observed in table 5. For the EDT oral group and TCA oral group, 11.80±0.37-13.4±0.48 mm and 11.86±0.27-13.2±0.14 mm have been observed, revealing a decrease in the volume of the joints in both groups after two weeks of treatment. 07.8±0.27-10.6±0.30 mm of joint volume for the EDTg group have been observed, showing the joint volume decreases significantly compared to the controlled group. For the TCAg group, a joint volume of 08.4±0.16–10.96±0.15 mm has been observed, depicting less volume than the animals in the controlled group. Therefore, a decrease in joint volume for the gel groups shows significant management of the joint swelling caused by OA induction before two weeks of treatment. As compared to the two drug-loaded gels, animals in the TCAg group showed a lower joint swelling index than those in the EDTg group.

Table 5: Joint swelling of Osteoarthritis induced rats of different groups

Groups animals	Control (mm)	EDT oral (mm)	TCA oral (mm)	EDTg (mm)	TCAg (mm)
1	13.5±0.37	13.4±0.48	12.58±0.24	10.24±0.28	08.86±0.18
2	13±0.35	12.4±0.24	12.48±0.45	09.5±0.26	08.58±0.16
3	12.8±0.29	11.8±0.37	11.86±0.27	09.45±0.24	09.76±0.05
4	13.8±0.43	13.3±0.35	12.98±0.25	10.6±0.30	10.96±0.15
5	13.6±0.38	12.8±0.24	13.2±0.14	08.7±0.36	08.4±0.16
6	12±0.32	11.9±0.19	11.98±0.29	07.8±0.27	08.8±0.04

Data represted as mean±SD, n = 3 observations

In fig. 13, the posterior view of the left knee (circled in red) has been depicted in the radiographs of the bone structure of the joints of the animals in the normal, controlled, EDT-oral suspension, EDTg, TCA-oral suspension, and TCAg groups. Radiographs depict no change in the joints for the normal group. For the controlled group, inflammation of the joints between the medial femur and medial tibial plateau was observed, indicating OA formation. Bone sclerosis, or subchondral bone cysts with stiffness, has been found in the joints treated with EDT suspensions and TCA suspensions through oral routes of administration. For the EDTg group, less osteophyte in the knee joints than in the control group has been observed. Less inflammation with the normal structure of the femur and the cartilage has been observed for the TCAg group. Overall, the X-ray radiographs proved the changes in the rat knee joints, as the treatment follows with EDT-NLCs and TCA-NLC-loaded gels.

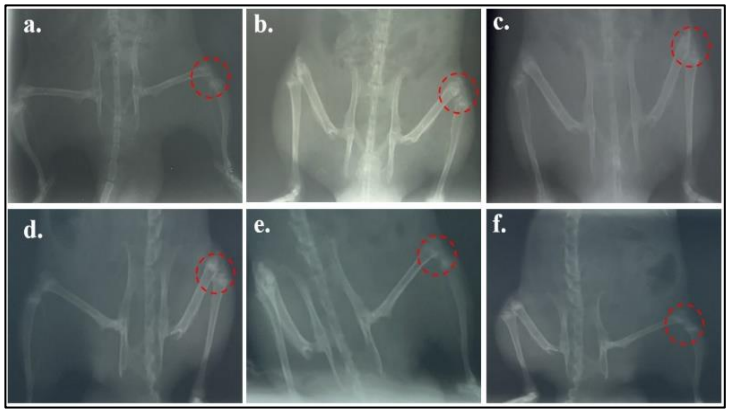

Fig. 13: X-ray images of the left knee of the animals in (a.) the normal group, (b.) the controlled group, (c.) the oral suspension of EDT, (d.) the oral suspension of TCA, (e.) the EDTg group, and (f.) the TCAg group

In fig. 14, the histopathological changes in the tissues of the knee joints, spleen, and skin of the rats of the normal group, the controlled group, the oral suspension of the EDT group and the TCA group, the EDTg group, and the TCAg group have been shown. For the normal group, normal morphology of the cartilage and the bone marrow structure has been observed for the knee joints. No demarcation between the red and white pulp, no loss of architecture, and no degenerative changes with cellular infiltration have been observed

in the spleen tissues of the normal group. For the joints of the controlled group, complete resorption of the bony trabecular region and partial replacement with connective tissue with osteoclast and osteoblast in the bone-forming cells have been observed. Multiple sites of the resorption region were also replaced with connective tissue. Structural integrity with red and white pulp and splenic cords with hyperplasia of cells have been observed for the spleen tissues. For the joint tissue of the oral suspension of the EDT group, severe hyperplastic changes in osteocytes with a loss of structural integrity of the tissue and a disintegrated muscular layer have been observed. Loss of spleen tissue architecture has also been observed with degenerative cells. Oral suspension in the TCA group, loss of tissue integrity with osteoblastic activity, vacuolation causing degenerative changes in the joints, and loss of spleen tissue architecture have been observed in this group. As the transdermal gels were only applied to the EDTg and TCAg groups, the skin tissues of the other groups revealed no loss of tissue integrity and no sign of cellular infiltration. Knee joint tissue for the EDTg group showed resorption of the bony trabecular region with complete replacement of osteoblast and the presence of connective tissue and fibrous tissue with proliferation. Damaged cartilage was replaced with connective tissue, and bone-forming cell signs were observed. The foci of the resorption site were also found to be replaced with mature bone. Structural integrity with red and white pulp and hypertrophic splenic cells with slight degenerative changes has been observed for the spleen tissues of this group. There was no loss of tissue architecture and the stratum layers for the skin tissue. Still, slight necrotic changes in the muscular layer and collagen have been found with minimal disintegration. For the TCAg group, the trabecular region in the bone has been completely replaced with bone-forming cells and connective tissue. A slight difference was observed in the spleen tissue compared to the oral group. There is a severe loss of architecture for the skin tissue, with a disintegrated stratum layer and connective collagen tissue. Although both gels showed a better effect on the joints and a lesser effect on the spleen tissue, TCAg showed degeneration of the skin tissue with a loss of tissue structure. For this reason, prepared EDTg is more potent for administering the drug to the patient.

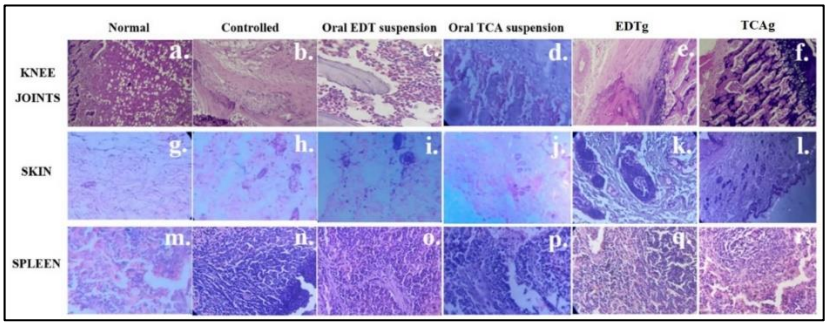

Fig. 14: Histopathological changes for the knee joints, spleen, and skin of the rats in different groups such as normal (a, g, m), controlled (b, h, n), oral suspension of EDT (c, i, o), oral suspension of TCA (d, j, p), EDTg (e, kq), and TCAg (f, l, r)

IHC observation for the knee joints of the rats of different groups of animals has been depicted in fig. 15, and the scoring of the immunoreactivity on different antibodies has been shown in fig. 16. The IHC staining identified no immune reactivity against IL-1β, IL-6, and TNF-α in lymphoid tissue for the normal group. In contrast, more than 70 to 80% of immune reactivity against IL-1β and 90% of immune reactivity against IL-6 and TNF-α in lymphoid tissue have been observed for the controlled group. In the case of the EDTg group, 10 to 20% immune reactivity against the IL-1 β antibodies has been observed. The cells were expressed in the inflammatory cells present in the cartilage, connective tissue, and pannus formation sites. The expression has been found in the myeloid precursor cells [neutrophils] and lymphoid precursor cells [lymphocytes] in bone marrow, present inside bony trabeculae. EDTg also showed 20 to 30% immune reactivity against IL-6 and TNF-α antibodies in cartilage, connective tissue, and pannus formation sites, especially in connective tissue and cartilage of the joints. The TCAg showed 10 to 20% immune reactivity against IL-1 in myeloid precursor cells [neutrophils] and lymphoid precursor cells [lymphocytes] in the bone marrow and the bony trabeculae.

Similarly, very little immune reactivity has been observed against IL-6 and TNF-α in myeloid precursor cells [neutrophils] and lymphoid precursors [lymphocytes] in bone marrow inside bony trabeculae. These results prove that the EDTg and TCAg showed less immune reactivity against the three antibodies than the control group. With less immune reactivity among the three antibodies, TCAg can be used as a better treatment method for osteoarthritis in the joints than EDTg.

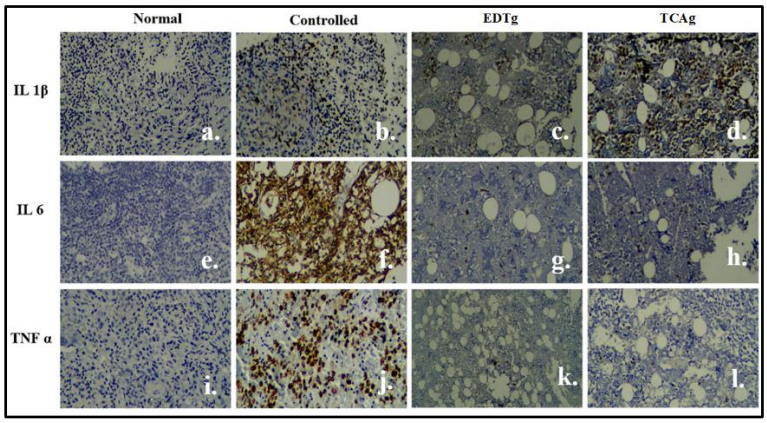

Fig. 15: IHC observation for IL 1β, IL 6 and TNF α antibodies expression for normal (a, e, i), controlled (b, f, j), EDTg (c, g, k) and TCAg (d, h, l) groups

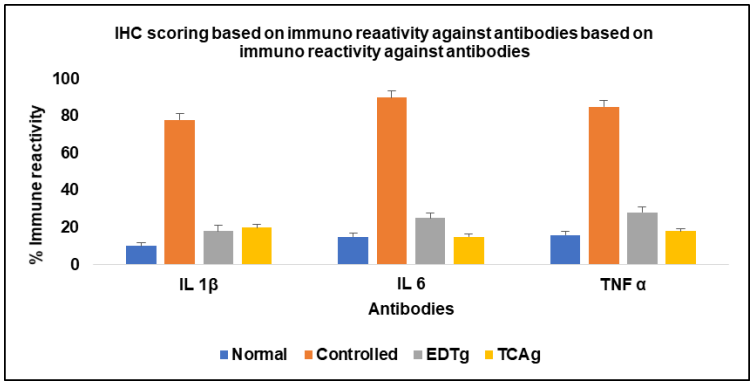

Fig. 16: An unbiased semi-quantitative scoring for the immunoreactivity of the IHC-stained sections for normal, controlled, EDTg and TCAg groups. The scale shows minimal (0) to maximum expression (100) against the antibodies, data represted as mean±SD, n = 3 observations

CONCLUSION

Successful incorporation of EDT and TCA drugs into NLCs has been done, and hydrogels have been prepared after the evaluation tests of the NLCs. The effectivity of the hydrogels has been measured by applying them to OA-induced Wistar rats to compare the effects of drugs released through gels and the oral route. Hence, findings from this study suggested that prepared EDTg can be used or can be considered as a better option for the management of OA pain than TCAg, surpassing any type of GIT irritation and also being convenient for the patient for the management of OA.

FUNDING

Nil

AUTHORS CONTRIBUTIONS

All the authors have discussed the results and contributed to the final manuscript. Souvik Chakraborty developed and performed the experiments, analysed the data and wrote the manuscript. N Vishal Gupta and Vikas Gupta contributed to the final version of the manuscript and supervised the project. Balamuralidhara V has been reviewed the manuscript.

CONFLICTS OF INTERESTS

All authors have none to declare

REFERENCES

1. Anandacoomarasamy A, March L. Current evidence for osteoarthritis treatments. Ther Adv Musculoskelet Dis. 2010 Feb;2(1):17-28. doi: 10.1177/1759720X09359889, PMID 22870434.
2. Boer CG, Hatzikotoulas K, Southam L, Stefansdottir L, Zhang Y, Coutinho de Almeida R. Deciphering osteoarthritis genetics across 826,690 individuals from 9 populations. Cell. 2021;184(18):4784-818.e17. doi: 10.1016/j.cell.2021.07.038.
3. Wieland HA, Michaelis M, Kirschbaum BJ, Rudolphi KA. Osteoarthritis-an untreatable disease? Nat Rev Drug Discov. 2005;4(4):331-44. doi: 10.1038/nrd1693, PMID 15803196.
4. Bannuru RR, Osani MC, Vaysbrot EE, Arden NK, Bennell K, Bierma Zeinstra SM. OARSI guidelines for the non-surgical management of knee, hip, and polyarticular osteoarthritis. Osteoarthritis Cartilage. 2019;27(11):1578-89. doi: 10.1016/j.joca.2019.06.011, PMID 31278997.
5. Kolasinski SL, Neogi T, Hochberg MC, Oatis C, Guyatt G, Block J. American college of rheumatology/arthritis foundation guideline for the management of osteoarthritis of the hand, hip, and knee. Arthritis Rheumatol. 2020;72(2):220-33. doi: 10.1002/art.41142, PMID 31908163.
6. Hochberg MC, Altman RD, April KT, Benkhalti M, Guyatt G, McGowan J. American college of rheumatology 2012 recommendations for the use of nonpharmacologic and pharmacologic therapies in osteoarthritis of the hand, hip, and knee. Arthritis Care Res (Hoboken). 2012;64(4):465-74. doi: 10.1002/acr.21596, PMID 22563589.
7. Jordan KM, Arden NK, Doherty M, Bannwarth B, Bijlsma JW, Dieppe P. Eular recommendations 2003: an evidence-based approach to the management of knee osteoarthritis: report of a task force of the standing committee for international clinical studies including therapeutic trials (ESCISIT). Ann Rheum Dis. 2003;62(12):1145-55. doi: 10.1136/ard.2003.011742, PMID 14644851.
8. McAlindon TE, Bannuru RR, Sullivan MC, Arden NK, Berenbaum F, Bierma-Zeinstra SM. OARSI guidelines for the non-surgical management of knee osteoarthritis. Osteoarthritis Cartilage. 2014;22(3):363-88. doi: 10.1016/j.joca.2014.01.003, PMID 24462672.
9. Da Costa BR, Pereira TV, Saadat P, Rudnicki M, Iskander SM, Bodmer NS. Effectiveness and safety of non-steroidal anti-inflammatory drugs and opioid treatment for knee and hip osteoarthritis: network meta-analysis. BMJ. 2021;375:n2321. doi: 10.1136/bmj.n2321, PMID 34642179.
10. Scarpignato C, Lanas A, Blandizzi C, Lems WF, Hermann M, Hunt RH. Safe prescribing of non-steroidal anti-inflammatory drugs in patients with osteoarthritis-an expert consensus addressing benefits as well as gastrointestinal and cardiovascular risks. BMC Med. 2015;13:55. doi: 10.1186/s12916-015-0285-8, PMID 25857826.
11. Zeng C, Wei J, Persson MS, Sarmanova A, Doherty M, Xie D. Relative efficacy and safety of topical non-steroidal anti-inflammatory drugs for osteoarthritis: a systematic review and network meta-analysis of randomised controlled trials and observational studies. Br J Sports Med. 2018;52(10):642-50. doi: 10.1136/bjsports-2017-098043, PMID 29436380.
12. Hochberg MC, Altman RD, Brandt KD, Clark BM, Dieppe PA, Griffin MR. Guidelines for the medical management of osteoarthritis. Part II. Osteoarthritis of the knee. American College of Rheumatology. Arthritis Rheum. 1995;38(11):1541-6. doi: 10.1002/art.1780381104, PMID 7488273.
13. Zhang Y, Cun D, Kong X, Fang L. Design and evaluation of a novel transdermal patch containing diclofenac and teriflunomide for rheumatoid arthritis therapy. Asian J Pharm Sci. 2014;9(5):251-9. doi: 10.1016/j.ajps.2014.07.007.
14. Von Heideken J, Chowdhry S, Borg J, James K, Iversen MD. Reporting of harm in randomized controlled trials of therapeutic exercise for knee osteoarthritis: a systematic review. Phys Ther. 2021;101(10):161. doi: 10.1093/ptj/pzab161, PMID 34180534.
15. Abdellatif AA, El-Telbany DF, Zayed G, Al-Sawahli MM. Hydrogel containing PEG-coated fluconazole nanoparticles with enhanced solubility and antifungal activity. J Pharm Innov. 2019;14(2):112-22. doi: 10.1007/s12247-018-9335-z.
16. Karadzovska D, Brooks JD, Riviere JE. Modeling the effect of experimental variables on the *in vitro* permeation of six model compounds across porcine skin. Int J Pharm. 2013;443(1-2):58-67. doi: 10.1016/j.ijpharm.2013.01.002, PMID 23313919.
17. Kurakula M, Ahmed OA, Fahmy UA, Ahmed TA. Solid lipid nanoparticles for transdermal delivery of avanafil: optimization,

formulation, *in vitro* and ex-vivo studies. J Liposome Res. 2016;26(4):288-96. doi: 10.3109/08982104.2015.1117490, PMID 26784833.

18. Schnitzer TJ, Ballard IM, Constantine G, McDonald P. Double-blind, placebo-controlled comparison of the safety and efficacy of orally administered etodolac and nabumetone in patients with active osteoarthritis of the knee. Clin Ther. 1995;17(4):602-12. doi: 10.1016/0149-2918(95)80037-9, PMID 8565024.
19. Van Middelkoop M, Arden NK, Atchia I, Birrell F, Chao J, Rezende MU. The OA Trial bank: a meta-analysis of individual patient data from knee and hip osteoarthritis trials show that patients with severe pain exhibit greater benefit from intra-articular glucocorticoids. Osteoarthritis Cartilage. 2016;24(7):1143-52. doi: 10.1016/j.joca.2016.01.983, PMID 26836288.
20. Xing D, Yang Y, Ma X, Ma J, Ma B, Chen Y. Dose intraarticular steroid injection increase the rate of infection in subsequent arthroplasty: grading the evidence through a meta-analysis. J Orthop Surg Res. 2014;9:107. doi: 10.1186/s13018-014-0107-2, PMID 25391629.
21. Mohammadi M, Pezeshki A, Mesgari Abbasi M, Ghanbarzadeh B, Hamishehkar H. Vitamin D3-loaded nanostructured lipid carriers as a potential approach for fortifying food beverages; *in vitro* and *in vivo* evaluation. Adv Pharm Bull. 2017;7(1):61-71. doi: 10.15171/apb.2017.008, PMID 28507938.
22. Radha GV, Sastri KT, Prathyusha P, Bhanu P, Rajkumar J. Formulation and evaluation of aceclofenac proniosome loaded orabase for management of dental pain. Int J App Pharm. 2018;10(6):204-10. doi: 10.22159/ijap.2018v10i6.29143.
23. Kumar G, Sushma B, Jeyaprakash M. LC-MS/MS-based quantitative profiling of papain enzyme in carica papaya L.: method development and validation. Int J Appl Pharm. 2024;16(2):86-91.
24. Iqbal B, Ali J, Baboota S. Silymarin loaded nanostructured lipid carrier: from design and dermatokinetic study to mechanistic analysis of epidermal drug deposition enhancement. J Mol Liq. 2018;255:513-29. doi: 10.1016/j.molliq.2018.01.141.
25. Patel DK, Kesharwani R, Kumar V. Etodolac loaded solid lipid nanoparticle-based topical gel for enhanced skin delivery. Biocatal Agric Biotechnol. 2020;29:101810. doi: 10.1016/j.bcab.2020.101810.
26. Kawadkar J, Pathak A, Kishore R, Chauhan MK. Formulation, characterization and *in vitro–in vivo* evaluation of flurbiprofen-loaded nanostructured lipid carriers for transdermal delivery. Drug Dev Ind Pharm. 2013;39(4):569-78. doi: 10.3109/03639045.2012.686509, PMID 22639934.
27. Chand P, Kumar H, Badduri N, Gupta NV, Bettada VG, Madhunapantula SV. Design and evaluation of cabazitaxel-loaded NLCs against breast cancer cell lines. Colloids Surf B Biointerfaces. 2021;199:111535. doi: 10.1016/j.colsurfb.2020.111535, PMID 33360926.
28. Mohammadi Samani S, Zojaji S, Entezar Almahdi E. Piroxicam loaded solid lipid nanoparticles for topical delivery: preparation, characterization and *in vitro* permeation assessment. J Drug Deliv Sci Technol. 2018;47:427-33. doi: 10.1016/j.jddst.2018.07.015.
29. Jain K, Sood S, Gowthamarajan K. Optimization of artemether-loaded NLC for intranasal delivery using central composite design. Drug Deliv. 2015;22(7):940-54. doi: 10.3109/10717544.2014.885999, PMID 24512368.
30. Patel S, Shah UH. Synthesis of flavones from 2-hydroxy acetophenone and aromatic aldehyde derivatives by conventional methods and green chemistry approach. Asian J Pharm Clin Res 2017;10(2):403-6. doi: 10.22159/ajpcr.2017.v10i2.15928.
31. Hu FQ, Jiang SP, Du YZ, Yuan H, Ye YQ, Zeng S. Preparation and characterization of stearic acid nanostructured lipid carriers by solvent diffusion method in an aqueous system. Colloids Surf B Biointerfaces. 2005;45(3-4):167-73. doi: 10.1016/j.colsurfb.2005.08.005, PMID 16198092.
32. Wamorkar V, Varma MM, Manjunath SY. Formulation and evaluation of stomach-specific in-situ gel of metoclopramide using natural, bio-degradable polymers. Int J. Biomed Sci. 2011;2:193-201.
33. Zhuang CY, Li N, Wang M, Zhang XN, Pan WS, Peng JJ. Preparation and characterization of vinpocetine-loaded nanostructured lipid carriers (NLC) for improved oral bioavailability. Int J Pharm. 2010;394(1-2):179-85. doi: 10.1016/j.ijpharm.2010.05.005, PMID 20471464.
34. Luo Q, Zhao J, Zhang X, Pan W. Nanostructured lipid carrier (NLC) coated with chitosan oligosaccharides and its potential use in ocular drug delivery system. Int J Pharm. 2011;403(1-2):185-91. doi: 10.1016/j.ijpharm.2010.10.013, PMID 20951778.
35. Shah NV, Seth AK, Balaraman R, Aundhia CJ, Maheshwari RA, Parmar GR. Nanostructured lipid carriers for oral bioavailability enhancement of raloxifene: design and *in vivo* study. J Adv Res. 2016;7(3):423-34. doi: 10.1016/j.jare.2016.03.002, PMID 27222747.
36. He Y, Majid K, Maqbool M, Hussain T, Yousaf AM, Khan IU. Formulation and characterization of lornoxicam-loaded cellulosic-microsponge gel for possible applications in arthritis. Saudi Pharm J. 2020;28(8):994-1003. doi: 10.1016/j.jsps.2020.06.021, PMID 32792844.
37. Souto EB, Wissing SA, Barbosa CM, Müller RH. Evaluation of the physical stability of SLN and NLC before and after incorporation into hydrogel formulations. Eur J Pharm Biopharm. 2004;58(1):83-90. doi: 10.1016/j.ejpb.2004.02.015, PMID 15207541.
38. Bove SE, Calcaterra SL, Brooker RM, Huber CM, Guzman RE, Juneau PL. Weight-bearing as a measure of disease progression and efficacy of anti-inflammatory compounds in a model of monosodium iodoacetate-induced osteoarthritis. Osteoarthritis Cartilage. 2003;11(11):821-30. doi: 10.1016/s1063-4584(03)00163-8, PMID 14609535.
39. Patel KN, Patel HK, Patel VA. Formulation and characterization of drug in adhesive transdermal patches of diclofenac acid. Int J Pharm Pharm Sci. 2012;4:296-9.
40. Vashisth I, Ahad A, Aqil M, Agarwal SP. Investigating the potential of essential oils as penetration enhancer for transdermal losartan delivery: effectiveness and mechanism of action. Asian J Pharm Sci. 2014;9(5):260-7. doi: 10.1016/j.ajps.2014.06.007.
41. Danafar H, Hamidi M. Simple and sensitive high-performance liquid chromatography (HPLC) method with UV detection for mycophenolic acid assay in human plasma. Application to a bioequivalence study. Adv Pharm Bull. 2015;5(4):563-8. doi: 10.15171/apb.2015.076, PMID 26819930.
42. Liu SC, Lee HP, Hung CY, Tsai CH, Li TM, Tang CH. Berberine attenuates CCN2-induced IL-1β expression and prevents cartilage degradation in a rat model of osteoarthritis. Toxicol Appl Pharmacol. 2015;289(1):20-9. doi: 10.1016/j.taap.2015.08.020, PMID 26344001.
43. Bhalekar MR. Solid lipid nanoparticles incorporated transdermal patch for improving the permeation of piroxicam. Asian J Pharm. 2016;10(1):45-50.
44. Ah YC, Choi JK, Choi YK, Ki HM, Bae JH. A novel transdermal patch incorporating meloxicam: *in vitro* and *in vivo* characterization. Int J Pharm. 2010;385(1-2):12-9. doi: 10.1016/j.ijpharm.2009.10.013, PMID 19833177.
45. Sun L, Cun D, Yuan BO, Cui H, Xi H, Mu L. Formulation and *in vitro*/*in vivo* correlation of a drug-in-adhesive transdermal patch containing azasetron. J Pharm Sci. 2012;101(12):4540-8. doi: 10.1002/jps.23317, PMID 22972714.
46. Sastri KT, Gupta NV, Kannan A, Balamuralidhara V, Ramkishan A. Potential nanocarrier-mediated miRNA-based therapy approaches for multiple sclerosis. Drug Discov Today. 2022;27:103357.
47. C Juneja S, Ventura M. A less invasive approach of medial meniscectomy in rat: a model to target early or less severe human osteoarthritis. J Arthritis. 2016;05(2):1-17. doi: 10.4172/2167-7921.1000193.
48. Mishra N, Mishra M, Padh H. Formulation development and optimization of efavirenz loaded SLNs and NLCs using placket-burman design and its statistical elucidation. Int J Pharm R H Sci. 2018;6:2379-88.
49. Gonullu U, Uner M, Yener G, Karaman EF, Aydogmuş Z. Formulation and characterization of solid lipid nanoparticles, nanostructured lipid carriers and nanoemulsion of lornoxicam for transdermal delivery. Acta Pharm. 2015;65(1):1-13. doi: 10.1515/acph-2015-0009, PMID 25781700.
50. Li X, Nie SF, Kong J, Li N, Ju CY, Pan WS. A controlled-release ocular delivery system for ibuprofen based on nanostructured

lipid carriers. Int J Pharm. 2008;363(1-2):177-82. doi: 10.1016/j.ijpharm.2008.07.017, PMID 18706987.

51. Unger WW, van Beelen AJ, Bruijns SC, Joshi M, Fehres CM, van Bloois L. Glycan-modified liposomes boost CD4+ and CD8+ T-cell responses by targeting DC-SIGN on dendritic cells. J Control Release. 2012;160(1):88-95. doi: 10.1016/j.jconrel.2012.02.007, PMID 22366522.
52. Jain V, Kumar H, Chand P, Jain S. Lipid-based nanocarriers as drug delivery system and its applications. Nanopharmaceutical Adv Deliv Syst. 2021:1-29.
53. Dandagi PM, Dessai GA, Gadad AP, Desai VB. Formulation and evaluation of nanostructured lipid carrier (NLC) of lornoxicam. Int J Pharm Pharm Sci. 2014;6(2):73-7.
54. Kumar RM, Kumar H, Bhatt T, Jain R, Panchal K, Chaurasiya A. Fisetin in cancer: attributes, developmental aspects, and nanotherapeutics. Pharmaceuticals (Basel). 2023;16(2):196. doi: 10.3390/ph16020196, PMID 37259344.
55. Bhattacharya SA, Prajapati BG. Formulation and optimization of celecoxib nanoemulgel. Asian J Pharm Clin Res. 2017;10(8):353-65. doi: 10.22159/ajpcr.2017.v10i8.19510.
56. Gaba B, Fazil M, Khan S, Ali A, Baboota S, Ali J. Nanostructured lipid carrier system for topical delivery of terbinafine hydrochloride. Bull Fac Pharm Cairo Univ. 2015;53(2):147-59. doi: 10.1016/j.bfopcu.2015.10.001.
57. Kumar H, Chand P, Pachal S, Mallick S, Jain R, Madhunapantula SV. Fisetin-loaded nanostructured lipid carriers: formulation and evaluations against advanced and metastatic melanoma. Mol Pharm. 2023;20(12):6035-55. doi: 10.1021/acs.molpharmaceut.3c00309, PMID 37906601.
58. Shah JI, Patel SH, Bhairy SR, Hirlekar RA. Formulation optimization, characterization and *in vitro* anti-cancer activity of curcumin loaded nanostructured lipid carriers. Int J Curr Pharm Sci. 2022;14(1):31-43. doi: 10.22159/ijcpr.2022v14i1.44110.
59. Abdelbary G, Haider M. *In vitro* characterization and growth inhibition effect of nanostructured lipid carriers for controlled delivery of methotrexate. Pharm Dev Technol. 2013;18(5):1159-68. doi: 10.3109/10837450.2011.614251, PMID 21958084.
60. Chakraborty S, Gupta NV, Sastri KT, MS, Chand P, Kumar H. Current progressions in transdermal drug delivery systems for management of rheumatoid and osteoarthritis: a comprehensive review. J Drug Deliv Sci Technol. 2022;73:103476. doi: 10.1016/j.jddst.2022.103476.